

# Numerical simulation of forced convection heat transfer from a cylinder with high conductivity radial fins in cross-flow

Bassam A/K Abu-Hijleh

*School of Aerospace, Mechanical and Manufacturing Engineering, RMIT University, Bundoora, Victoria 3083, Australia*

Received 4 February 2002; accepted 18 October 2002

## Abstract

The problem of cross-flow forced convection heat transfer from a horizontal cylinder with multiple equally spaced high conductivity radial fins on its outer surface was investigated numerically. The effect of several combinations of number of fins and fin height on the average Nusselt number was studied over the range of Reynolds number (1–200). The results showed that there was an optimum number of fins to obtain the maximum Nusselt number for a given value of fin height and Reynolds number. Short fins ( $H \leq 0.1$ ) slightly decreased the Nusselt number. A large number of long fins reduced the Nusselt number at the top range of Reynolds number studied.

© 2003 Éditions scientifiques et médicales Elsevier SAS. All rights reserved.

## 1. Introduction

Laminar forced convection across a heated cylinder is an important problem in heat transfer. It is used to simulate a wide range of engineering applications as well as provide a better insight into more complex systems of heat transfer. Accurate knowledge of the convection heat transfer around circular cylinders is important in many fields, including heat exchangers, hot water and steam pipes, heaters, refrigerators and electrical conductors. Because of its industrial importance, this class of heat transfer has been the subject of many experimental and analytical studies. Though a lot of work has been done in this area, it still remains the subject of many investigations. Recent economic and environmental concerns have raised the interest in methods of increasing or reducing the convection heat transfer, depending on the application, from a horizontal cylinder. Researchers continue to look for new methods of heat transfer control. The use of porous materials to alter the heat transfer characteristics has been reported by several researchers including Vafai and Huang [1], Al-Nimr and Alkam [2], and Abu-Hijleh [3].

This paper presents the numerical results of using high conductivity fins on the cylinder's outer surface in order to enhance the forced convection heat transfer from a cylinder in cross-flow. The fluid under consideration is air. The

numerical solution of the elliptic momentum and energy equations was performed using the stream function-vorticity method on a stretched grid [4]. This detailed study included varying the Reynolds number from 1 to 200, number of fins from 0 to 18, and the non-dimensional fin height from 0.05 to 3.

## 2. Mathematical analysis

The steady-state equations for 2-D laminar forced convection over a horizontal cylinder are given by:

$$\frac{1}{r} \frac{\partial(ru)}{\partial r} + \frac{1}{r} \frac{\partial v}{\partial \theta} = 0 \quad (1)$$

$$\begin{aligned} u \frac{\partial u}{\partial r} + \frac{v}{r} \frac{\partial u}{\partial \theta} - \frac{v^2}{r} \\ = -\frac{1}{\rho} \frac{\partial p}{\partial r} + \nu \left[ \frac{\partial^2 u}{\partial r^2} + \frac{1}{r} \frac{\partial u}{\partial r} - \frac{u}{r^2} + \frac{1}{r^2} \frac{\partial^2 u}{\partial \theta^2} - \frac{2}{r^2} \frac{\partial v}{\partial \theta} \right] \end{aligned} \quad (2)$$

$$\begin{aligned} u \frac{\partial v}{\partial r} + \frac{v}{r} \frac{\partial v}{\partial \theta} + \frac{uv}{r} \\ = -\frac{1}{\rho} \frac{\partial p}{\partial \theta} + \nu \left[ \frac{\partial^2 v}{\partial r^2} + \frac{1}{r} \frac{\partial v}{\partial r} - \frac{v}{r^2} + \frac{1}{r^2} \frac{\partial^2 v}{\partial \theta^2} + \frac{2}{r^2} \frac{\partial u}{\partial \theta} \right] \end{aligned} \quad (3)$$

$$u \frac{\partial T}{\partial r} + \frac{v}{r} \frac{\partial T}{\partial \theta} = \alpha \nabla^2 T \quad (4)$$

*E-mail address:* bassam.abu-hijleh@rmit.edu.au (B. A/K Abu-Hijleh).

**Nomenclature**

$D$	cylinder diameter, $= 2r_o$ m
$E$	parameter in computational domain, $= \pi e^{\pi \xi}$
$F$	number of equally spaced fins
$g$	gravity ..... $\text{m}\cdot\text{s}^{-2}$
$H$	non-dimensional fin height, $= h_F/r_o$
$h$	local convection heat transfer coefficient ..... $\text{W}\cdot\text{m}^{-2}\text{K}^{-1}$
$h_F$	fin height ..... m
$k$	conduction heat transfer coefficient ..... $\text{W}\cdot\text{m}^{-1}\cdot\text{K}^{-1}$
$M$	number of grid points in the tangential direction
$N$	number of grid points in the radial direction
$Nu_D$	local Nusselt number based on cylinder diameter
$\overline{Nu_D}$	average Nusselt number based on cylinder diameter, no fins
$\overline{Nu_{D,F}}$	average Nusselt number based on cylinder diameter, cylinder with $F$ number of fins
$P$	non-dimensional pressure
$p$	pressure ..... Pa
$Pr$	Prandtl number
$R$	non-dimensional radius
$r$	radius ..... m
$Re$	Reynolds number based on cylinder radius, $= U_\infty r_o/\nu$
$Re_D$	Reynolds number based on cylinder diameter, $U_\infty D/\nu = 2Re$

$T$	temperature
$U$	non-dimensional radial velocity
$U_\infty$	incoming free stream velocity ..... $\text{m}\cdot\text{s}^{-1}$
$u$	radial velocity ..... $\text{m}\cdot\text{s}^{-1}$
$V$	non-dimensional tangential velocity
$v$	tangential velocity ..... $\text{m}\cdot\text{s}^{-1}$

*Greek symbols*

$\alpha$	thermal diffusivity ..... $\text{m}^2\cdot\text{s}^{-1}$
$\beta$	coefficient of thermal expansion ..... $\text{K}^{-1}$
$\varepsilon$	measure of convergence of numerical results
$\eta$	independent parameter in computational domain representing tangential direction
$\theta$	angle ..... degrees
$\nu$	kinematic viscosity ..... $\text{m}^2\cdot\text{s}^{-1}$
$\xi$	independent parameter in computational domain representing radial direction
$\rho$	density ..... $\text{kg}\cdot\text{m}^{-3}$
$\phi$	non-dimensional temperature
$\psi$	stream function
$\omega$	vorticity function

*Subscripts*

$D$	value based on cylinder diameter
$o$	value at cylinder surface
$\infty$	free stream value

where

$$\nabla^2 \equiv \left[ \frac{\partial^2}{\partial r^2} + \frac{1}{r} \frac{\partial}{\partial r} + \frac{1}{r^2} \frac{\partial^2}{\partial \theta^2} \right]$$

Eqs. (1)–(4) are subject to the following boundary conditions:

- (1) On the cylinder surface, i.e.,  $r = r_o$ ,  $u = v = 0$ , and  $T = T_o$ .
- (2) Far-stream from the cylinder, i.e.,  $r \rightarrow \infty$ ,  $u \rightarrow U_\infty \cos(\theta)$ , and  $v \rightarrow -U_\infty \sin(\theta)$ . As for the temperature, the far-stream boundary condition is divided into an outflow ( $\theta \leq 90$  degrees) and an inflow ( $\theta > 90$  degrees) regions, Fig. 1. The far-stream temperature boundary conditions are  $T = T_\infty$  and  $\partial T/\partial r = 0$  for the inflow and outflow regions, respectively.
- (3) Plane of symmetry;  $\theta = 0$  and  $\theta = 180$  degrees;  $v = 0$  and  $\partial u/\partial \theta = \partial T/\partial \theta = 0$ .
- (4) On the fin surface;  $u = v = 0$ . Since the fins are assumed to be very thin and of very high conductivity, the temperature at any point along the fin will be that of the cylinder surface, i.e.,  $T_F = T_o$ . The fins are equally spaced around the perimeter of the cylinder. No fins were placed at the horizontal line of symmetry, i.e., at  $\theta = 0$  and 180 degrees, see Fig 2.

The local Nusselt number, based on diameter, on the cylinder surface is given by:

$$Nu_D(\theta) = \frac{Dh(\theta)}{k} = -\frac{D}{(T_o - T_\infty)} \frac{\partial T(r_o, \theta)}{\partial r} \tag{5}$$

The local Nusselt number at fin, based on diameter, is given by:

$$Nu_{f,D}(\theta) = \int_{r_o}^{h_F} -\frac{D}{(T_o - T_\infty)} \frac{1}{r} \left[ \frac{\partial T(r, \theta)}{\partial r} \Big|_{\text{top}} + \frac{\partial T(r, \theta)}{\partial r} \Big|_{\text{bottom}} \right] dr \tag{6}$$

The following non-dimensional groups are introduced:

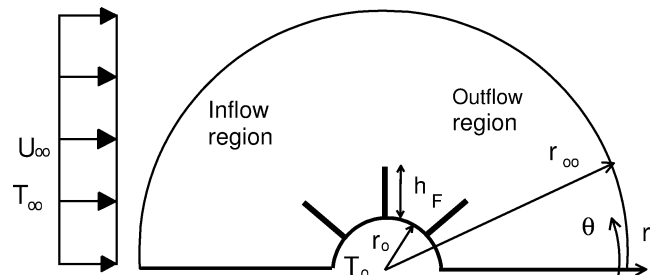


Fig. 1. Schematic diagram of the cylinder with equally spaced fins.

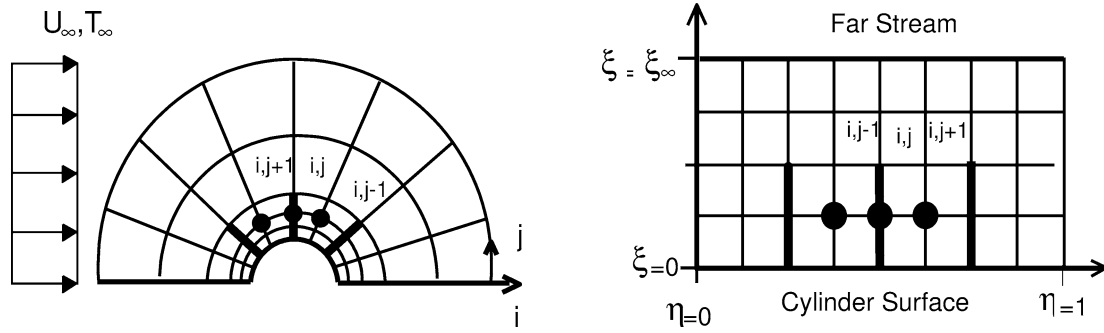


Fig. 2. Schematic diagram of the computational grid in the physical (left) and computational (right) domains.

$$R \equiv \frac{r}{r_o}, \quad U \equiv \frac{u}{U_\infty}, \quad V \equiv \frac{v}{U_\infty}$$

$$\phi \equiv \frac{(T - T_\infty)}{(T_o - T_\infty)}, \quad P \equiv \frac{(p - p_\infty)}{\frac{1}{2}\rho U_\infty^2}$$

Using the stream function–vorticity formulation, the non-dimensional form of Eqs. (1)–(4) are given by [4]:

$$\omega = \nabla^2 \psi \tag{7}$$

$$U \frac{\partial \omega}{\partial R} + \frac{V}{R} \frac{\partial \omega}{\partial \theta} = \frac{1}{Re} \nabla^2 \omega \tag{8}$$

$$U \frac{\partial \phi}{\partial R} + \frac{V}{R} \frac{\partial \phi}{\partial \theta} = \frac{1}{Re Pr} \nabla^2 \phi \tag{9}$$

where,

$$U \equiv \frac{1}{R} \frac{\partial \psi}{\partial \theta}, \quad V \equiv -\frac{\partial \psi}{\partial R} \tag{10}$$

$$Re = \frac{U_\infty r_o}{\nu}, \quad Re_D = \frac{U_\infty D}{\nu}, \quad Pr = \frac{\nu}{\alpha}$$

The new non-dimensional boundary conditions for Eqs. (7)–(9) are given by:

- (1) On the cylinder surface, i.e.,  $R = 1.0$ ,  $\psi = \partial\psi/\partial R = 0$ ,  $\omega = \partial^2\psi/\partial R^2$ , and  $\phi = 1.0$ .
- (2) Far-stream from the cylinder, i.e.,  $R \rightarrow \infty$ ,  $(\partial\psi/\partial R) = \sin(\theta)$ , and  $(1/R)(\partial\psi/\partial\theta) = \cos(\theta)$ . For the non-dimensional temperature,  $\phi = 0$  and  $\partial\phi/\partial R = 0$ , for the inflow and outflow regions, respectively.
- (3) Plane of symmetry;  $\psi = \omega = \partial\phi/\partial\theta = 0$ .
- (4) On the fin surface;  $\psi = 0$ ,  $\omega = (1/R^2)(\partial^2\psi/\partial\theta^2)$ , and  $\phi_{ij} = 1.0$ .

In order to accurately resolve the boundary layer around the cylinder, a grid with small radial spacing is required. It is not practical to use this small spacing as we move to the far-stream boundary. Thus a stretched grid in the radial direction is needed [4]. This will result in unequally spaced nodes and would require the use of more complicated and/or less accurate finite difference formulas. To overcome this problem, the unequally spaced grid in the physical domain  $(R, \theta)$  is transformed into an equally spaced grid in the computational domain  $(\xi, \eta)$  [4], Fig. 2. The two domains are related as follows:

$$R = e^{\pi\xi}, \quad \theta = \pi\eta \tag{11}$$

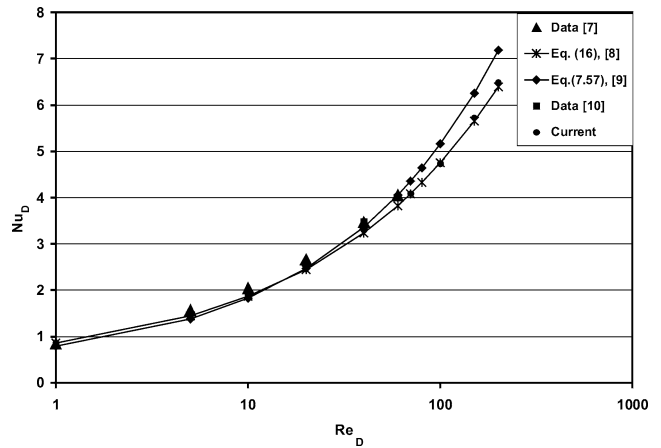


Fig. 3. Comparison of the local Nusselt number for the case of a smooth cylinder. The equations' numbers are from their respective references.

Eqs. (7)–(9) along with the corresponding boundary conditions need to be transformed into the computational domain. In the new computational domain, the current problem will be given by:

$$\omega = \frac{1}{E^2} \left[ \frac{\partial^2 \psi}{\partial \xi^2} + \frac{\partial^2 \psi}{\partial \eta^2} \right] \tag{12}$$

$$\frac{\partial^2 \omega}{\partial \xi^2} + \frac{\partial^2 \omega}{\partial \eta^2} = Re \left[ \frac{\partial \psi}{\partial \eta} \frac{\partial \omega}{\partial \xi} - \frac{\partial \psi}{\partial \xi} \frac{\partial \omega}{\partial \eta} \right] \tag{13}$$

$$\frac{\partial^2 \phi}{\partial \xi^2} + \frac{\partial^2 \phi}{\partial \eta^2} = Re Pr \left[ \frac{\partial \psi}{\partial \eta} \frac{\partial \phi}{\partial \xi} - \frac{\partial \psi}{\partial \xi} \frac{\partial \phi}{\partial \eta} \right] \tag{14}$$

where

$$E = \pi e^{\pi\xi} \tag{15}$$

The transformed boundary conditions are given by:

- (1) On the cylinder surface, i.e.,  $\xi = 0$ ,  $\psi = \partial\psi/\partial\xi = 0$ ,  $\omega = (1/\pi^2)(\partial^2\psi/\partial\xi^2)$ , and  $\phi = 1.0$ .
- (2) Far-stream from the cylinder, i.e.,  $\xi \rightarrow \infty$ ,  $\partial\psi/\partial\xi = E \sin(\theta)$ . In the inflow region;  $\omega = 0$  and  $\phi = 0$ . In the outflow region;  $\partial\omega/\partial\xi = 0$  and  $\partial\phi/\partial\xi = 0$ .
- (3) Plane of symmetry; i.e.,  $\eta = 0$  and  $\eta = 1$ ,  $\psi = \omega = \partial\phi/\partial\eta = 0$ .
- (4) On the fin surface;  $\psi = 0$ ,  $\omega = (1/E^2)(\partial^2\psi/\partial\eta^2)$ , and  $\phi_{ij} = 1.0$ .

The system of elliptic PDEs given by Eqs. (12)–(14) along with the corresponding boundary conditions was discretized using the finite difference method. The resulting system of algebraic equations was solved using the hybrid scheme [5]. Such a method proved to be numerically stable for convection-diffusion problems. The finite difference form of the equations was checked for consistency with the original PDEs [5]. The iterative solution procedure

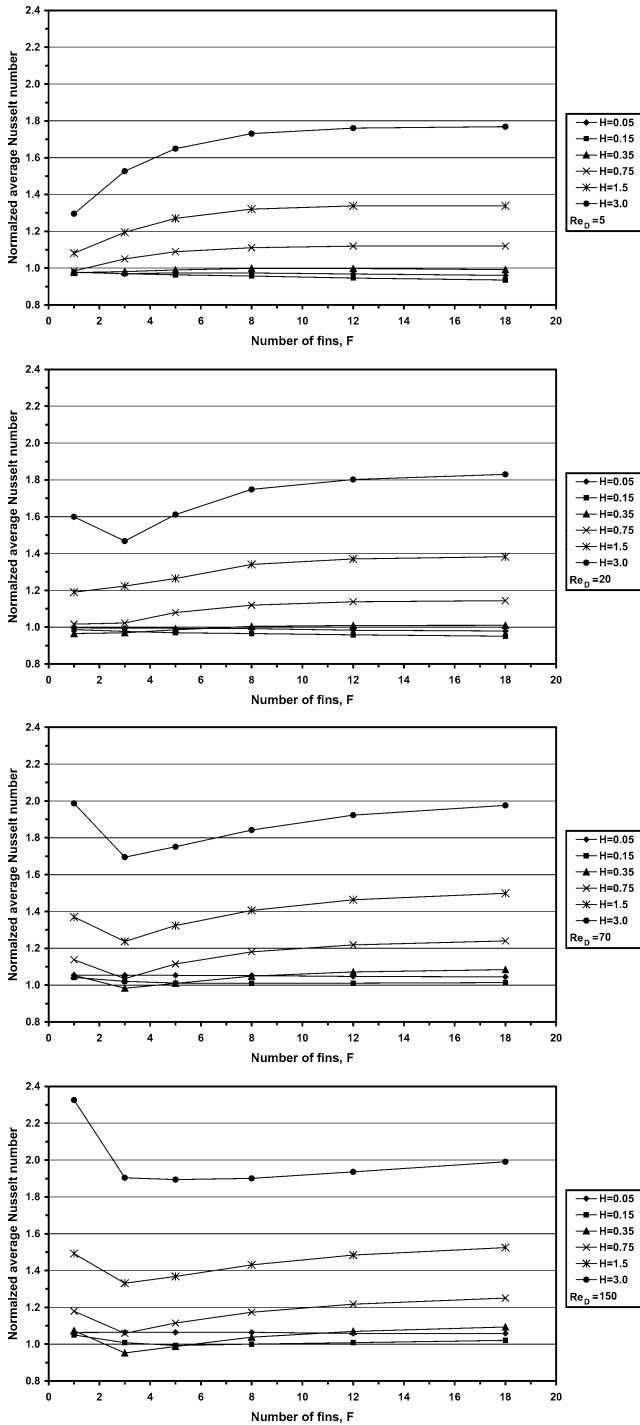


Fig. 4. Normalized average Nusselt number as a function of the number of fins at different combinations of fin height and  $Re_D$ .

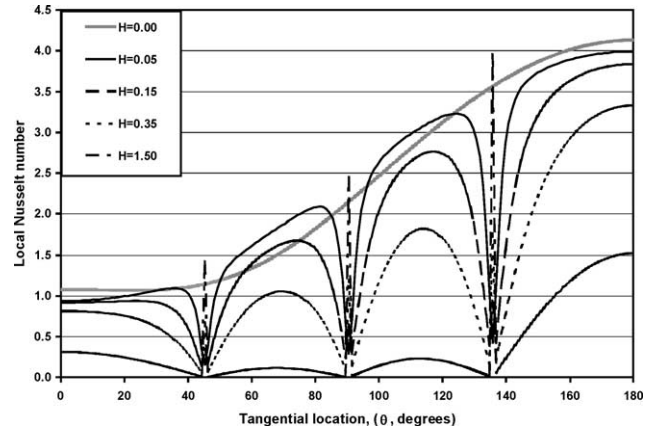


Fig. 5. Distribution of the local Nusselt number along the cylinder for the case of  $Re_D = 20$ ,  $F = 3$ , and  $H = 0.00$  (smooth cylinder, no fins), 0.05, 0.15, 0.35, 1.50.

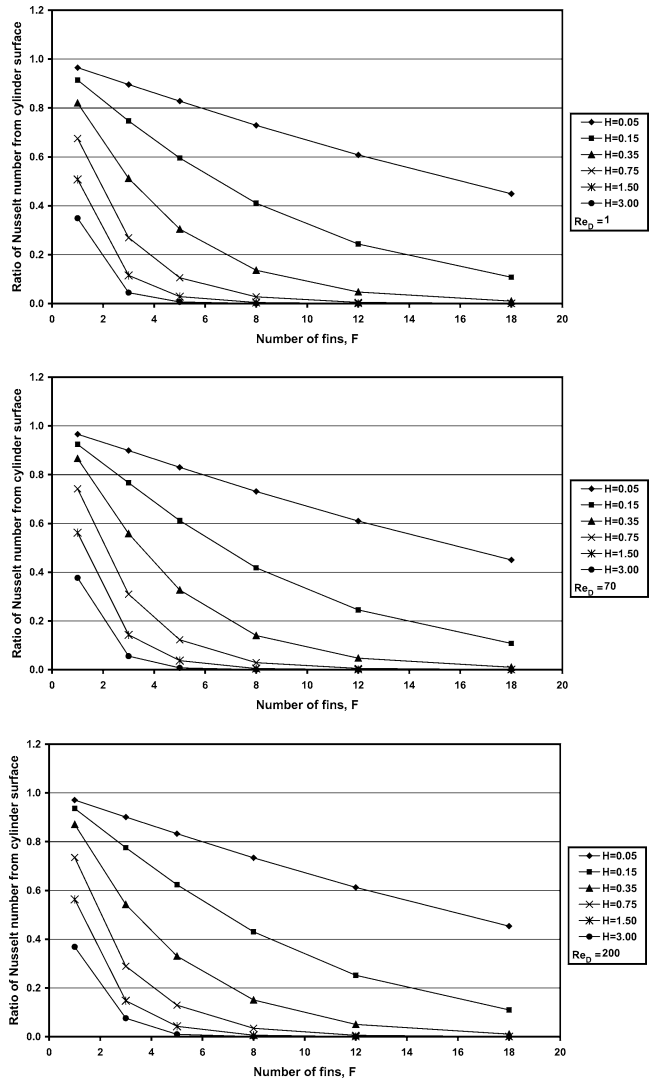


Fig. 6. Ratio of heat transfer from the cylinder surface, excluding the fins, to the total heat transfer from the cylinder at selective values of Reynolds number.

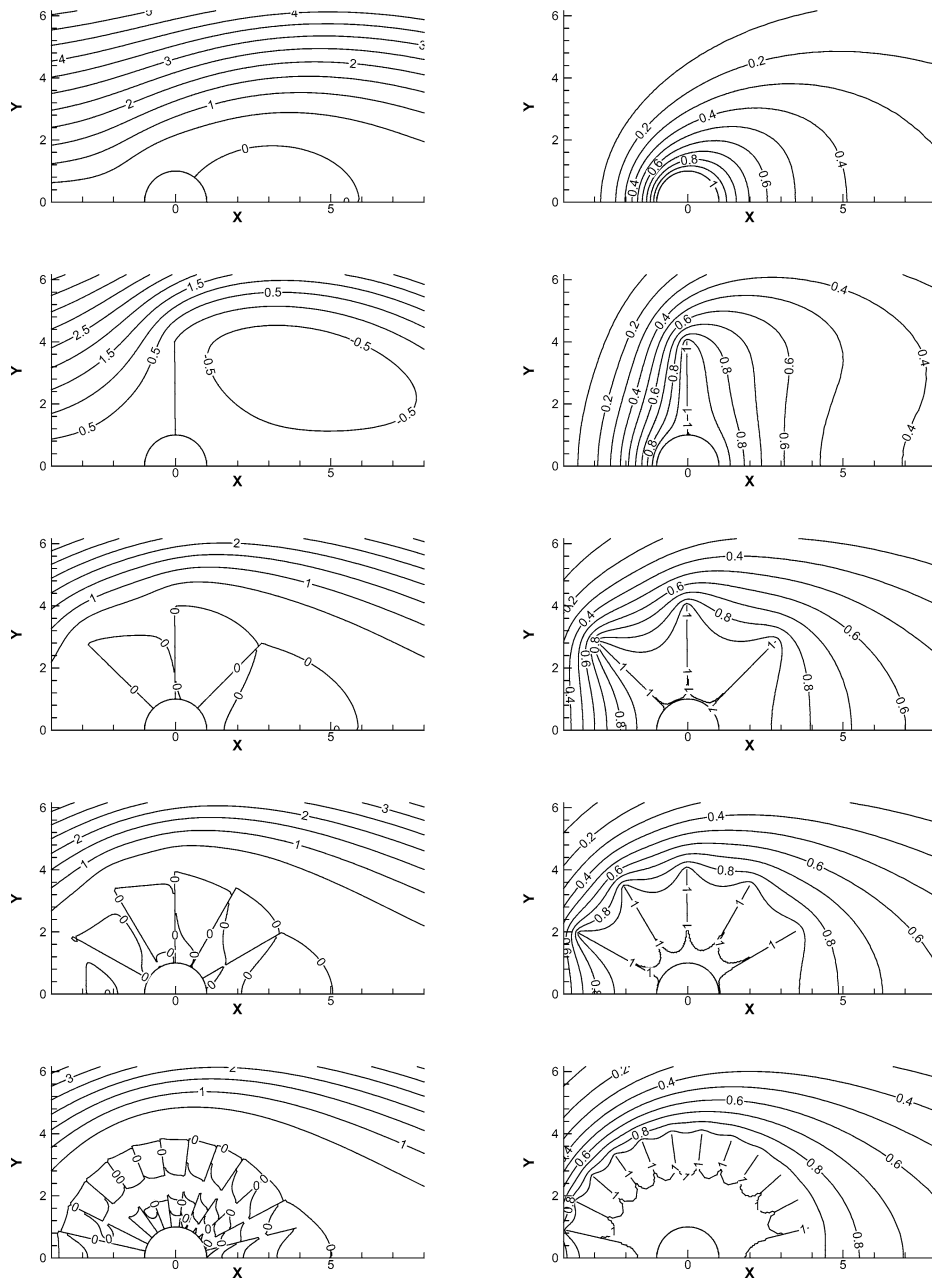


Fig. 7. Streamline (left) and isothermal (right) contours at  $Re_D = 5$ ,  $H = 3.00$ , and  $F = 0$  (smooth cylinder, no fins), 1, 3, 5, 12.

was carried out until the error in all solution variables ( $\psi$ ,  $\omega$ ,  $\phi$ ) became less than a predefined error level ( $\varepsilon$ ). Other predefined parameters needed for the solution method included the placement of the far-stream boundary condition ( $R_\infty$ ) and the number of grid points in both radial and tangential directions,  $N$  and  $M$ , respectively. Extensive testing was carried out in order to determine the effect of each of these parameters on the solution. This was done to ensure that the solution obtained was independent of and not tainted by the predefined value of each of these parameters. The testing included varying the value of  $\varepsilon$  from  $10^{-3}$  to  $10^{-6}$ ,  $R_\infty$  from 5 to 50,  $N$  from 100 to 200, and  $M$  from 120 to 200. The results reported herein

are based on the following combination:  $N = 150$ – $163$ ,  $M = 169$ – $180$ ,  $R_\infty = 15$ , and  $\varepsilon = 10^{-5}$ . Increasing any of these parameters resulted in minimal change ( $\leq 1\%$ ) in the computed Nusselt number. The variation in the number of grid points in the radial and tangential directions depended on fin number and fin height. The variation was to ensure that all fins coincided with one of the grid's radial lines and that the fins' end coincided with one of the grid's tangential lines, see Fig. 2. The current grid resolution is better than most grid resolutions used in published studies of natural [6], forced convection from a heated cylinder [7], and mixed convection at different angles of attack [8]. The large number of grid points in the tangential direction ( $M$ )

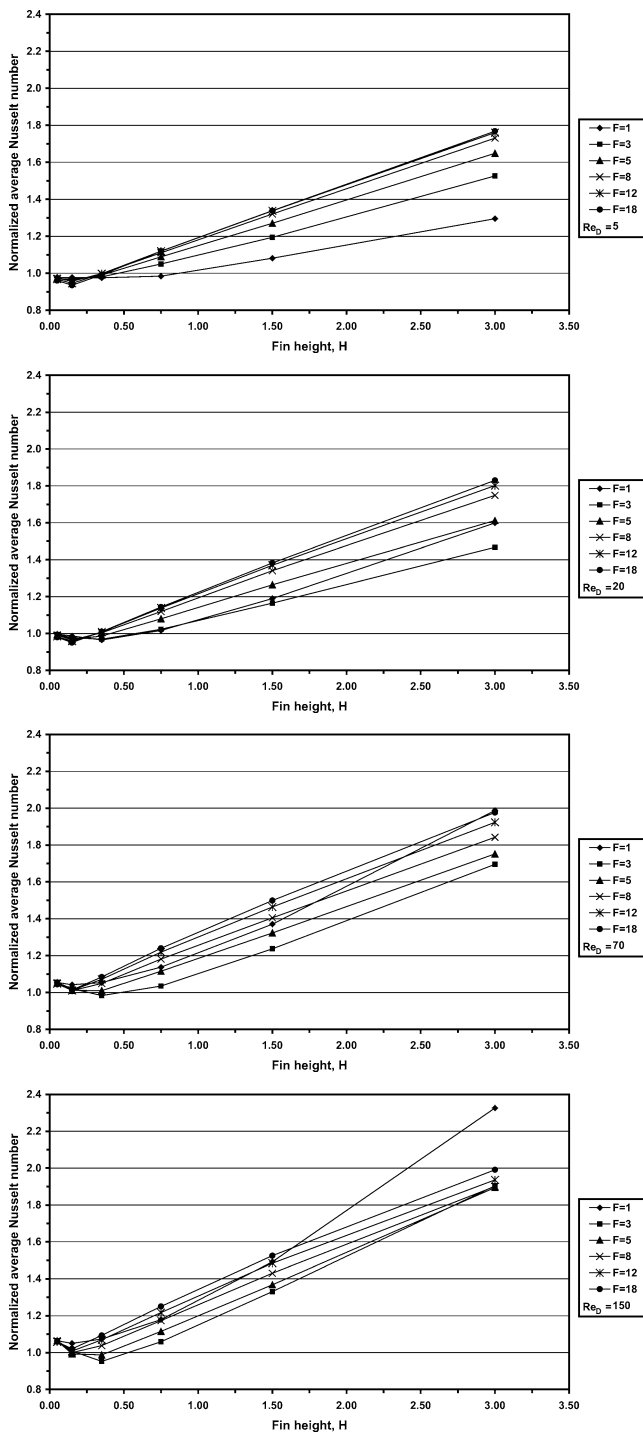


Fig. 8. Normalized average Nusselt number as a function of fin height for different number of fins and at different values of Reynolds number.

was to ensure that there were sufficient grid points between the fins to properly resolve the flow between the fins, even when using 18 fins. In comparison, the use of 60 points in the tangential direction would have been sufficient to resolve the flow around a smooth cylinder [8]. Fig. 3 shows very good agreement between the profiles of the average Nusselt number calculated by the current code and the several results

reported in the literature [7–10], for the case of a smooth cylinder with no fins.

### 3. Results

The effect of fins on the forced cross-flow heat transfer from a horizontal isothermal cylinder was studied for several combinations of number of fins ( $F = 1, 3, 5, 8, 12, 18$ ), non-dimensional fin height ( $H = 0.05, 0.15, 0.35, 0.75, 1.5, 3.0$ ), and Reynolds number ( $Re_D = 1, 5, 10, 20, 40, 70, 100, 150, 200$ ). The change in the average Nusselt number, for a given value of Reynolds number, due to the addition of  $F$  fin(s) ( $\overline{Nu}_{D,F}$ ) was normalized by the Nusselt number of a smooth cylinder, no fins, at the same Reynolds number ( $\overline{Nu}_D$ ). This was done in order to focus on the relative effect of adding the fins.

Fig. 4 shows the change in the normalized average Nusselt number as a function of number of fins at different values of fin height and selected Reynolds number. The change in the value of the normalized average Nusselt number ranged from  $-10\%$  to  $145\%$  depending on the number and height of the fins employed as well as the value of the Reynolds number. A small number of short fins tended to reduce the heat transfer from the cylinder. The addition of fins results in a reduction in the velocity of the air flow around the cylinder in the neighborhood of the fins. This in turn reduces the heat transfer from the cylinder surface. The extra heat transfer from the excess area gained due to the addition of these small fins did not compensate for the loss in the heat transfer from the cylinder surface resulting in a net reduction in the normalized average Nusselt number from the cylinder. When long fins are employed, the extra heat transfer from the much enlarged surface area more than compensates for the reduction in the heat transfer from the cylinder surface resulting in an increase in the normalized average Nusselt number. This can be seen clearly in Fig. 5 which shows the local Nusselt number distribution along the cylinder for the case of  $Re_D = 20$ ,  $F = 3$ , and  $H = 0.00$  (smooth cylinder, no fins),  $0.05, 0.15, 0.35, 1.50$ . At long fin heights, the heat transfer is predominantly from the fins with minimal contribution from the cylinder surface. This can be seen in Fig. 6 which shows the ratio of heat transfer from the cylinder surface, excluding the fins, to the total heat transfer from the cylinder at selective values of Reynolds number. An interesting feature from Fig. 6 is that the trend of the relative contribution of the cylinder surface area to the total heat transfer was almost universal, irrespective of the value of the Reynolds number.

Another observation from Fig. 4 is that there is an optimal number of fins for maximum increase in the normalized average Nusselt number, beyond which the addition of extra fins does not result in any enhancement of the convection heat transfer from the cylinder. Fig. 7 shows the streamline (left) and isothermal (right) contours for the case of  $Re_D = 5$ ,  $H = 3.0$ , and  $F = 0$  (smooth cylinder, no fins),

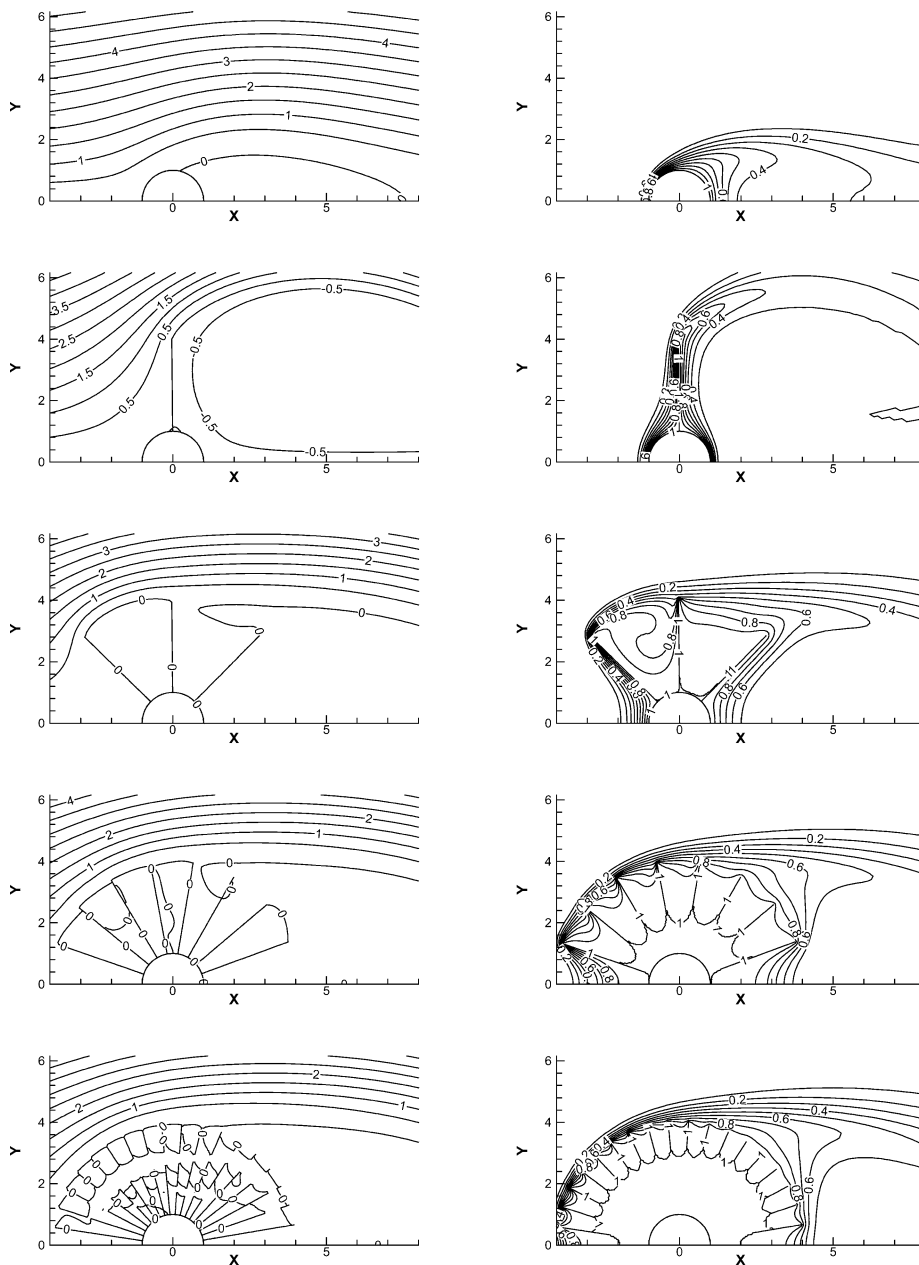


Fig. 9. Streamline (left) and isothermal (right) contours for the case  $Re_D = 150$ ,  $H = 3.00$ , and  $F = 0$  (smooth cylinder, no fins), 1, 3, 8, 18.

1, 3, 5, 12. From this figure, we can see that the fins form pockets of stagnant air between them. These pockets actually act as a buffer between the hot cylinder surface and the cold cross-flow air. The only active heat transfer area from the fin equipped cylinder is the top of the fins. As the number of fins increases, the buffer region between the fins increases. The increase in the number of fins is countered by a reduction in the active area per fin resulting in minimal, or as will be shown later a negative, change in the net heat transfer from the cylinder and resulting normalized average Nusselt number. This can be seen clearly from the last two fin combinations in Fig. 7.

Fig. 8 shows the change of the normalized average Nusselt number as a function of fin height for different

number of fins and at selected values of Reynolds number. The reduction in the normalized average Nusselt number due to short fins noted earlier in Figs. 4 and 5 is clearly visible in this figure. Fig. 8 also reveals another interesting trend. As the Reynolds number increases and when using long fins, a smaller number of fins is actually better in terms of dissipating heat from the cylinder than a larger number of similar fins. Fig. 9 shows the streamlines (left) and isothermal (right) contours for the case  $Re_D = 150$ ,  $H = 3.00$ , and  $F = 0$  (smooth cylinder, no fins), 1, 3, 8, 18. The large increase in the size of the stagnant air pocket due to the increase in the number of the long fins is clearly visible.

#### 4. Conclusions

The problem of cross-flow forced convection heat transfer from an isothermal horizontal cylinder with high conductivity equally spaced fins was studied numerically. Changes in the normalized average Nusselt number at different combinations of number of fins, fin height, and Reynolds number were reported. There was an optimum number of fins for maximum Nusselt number. Using more fins than the optimum number resulted in a reduction in Nusselt number. This number was fin height and Reynolds number dependent. Short fins slightly decreased the Nusselt number at low values of Reynolds number.

#### References

- [1] K. Vafai, P.C. Huang, Analysis of heat transfer regulation and modification employing intermittently emplaced porous cavities, *ASME J. Heat Transfer* 116 (1994) 604–613.
- [2] M.A. Al-Nimr, M.K. Alkam, A modified tubeless solar collector partially filled with porous substrate, *Renewable Energy* 13 (1998) 165–173.
- [3] B. A/K Abu-Hijleh, Natural convection heat transfer from a cylinder covered with an orthotropic porous layer, *J. Numer. Heat Transfer* 40 (2001) 421–443.
- [4] J.D. Anderson, *Computational Fluid Dynamics: The Basics with Applications*, McGraw-Hill, New York, 1994.
- [5] S.V. Patankar, *Numerical Heat Transfer and Fluid Flow*, McGraw-Hill, New York, 1980.
- [6] T. Saitoh, T. Sajik, K. Maruhara, Benchmark solutions to natural convection heat transfer problem around a horizontal circular cylinder, *Internat. J. Heat Mass Transfer* 36 (1993) 1251–1259.
- [7] R.A. Ahmad, Steady-state numerical solution of the Navier–Stokes and energy equations around a horizontal cylinder at moderate Reynolds numbers from 100 to 500, *Heat Transfer Engrg.* 17 (1996) 31–81.
- [8] B. A/K Abu-Hijleh, Laminar mixed convection correlations for an isothermal cylinder in cross flow at different angles of attack, *Internat. J. Heat Mass Transfer* 42 (1999) 1383–1388.
- [9] F.P. Incropera, D.P. DeWitt, *Fundamentals of Heat and Mass Transfer*, Wiley, New York, 1996.
- [10] H.M. Badr, A theoretical study of laminar mixed convection from a horizontal cylinder in a cross stream, *Internat. J. Heat Mass Transfer* 26 (1983) 639–653.